Thermoviscous-acoustic metamaterials to damp acoustic modes in complex shape geometries at low frequencies

Tenon Charly Kone, Maël Lopez, Sebastian Ghinet, et al.

Citation: The Journal of the Acoustical Society of America **150**, 2272 (2021); doi: 10.1121/10.0006441
View online: https://doi.org/10.1121/10.0006441
View Table of Contents: https://asa.scitation.org/toc/jas/150/3
Published by the Acoustical Society of America

JASA REVIEW-ARTICLE

Thermoviscous-acoustic metamaterials to damp acoustic modes in complex shape geometries at low frequencies

Tenon Charly Kone,[1,a)] Maël Lopez,[2] Sebastian Ghinet,[1] Thomas Dupont,[2,b)] and Raymond Panneton[3,c)]
[1]*Flight Research Laboratory, National Research Council Canada, 1200 Montreal Road, Ottawa, Ontario, K1A 0R6, Canada*
[2]*Department of Mechanical Engineering, École de Technologie Supérieure, 1100 Rue Notre-Dame Ouest, Montréal, Québec H3C 1K3, Canada*
[3]*Department of Mechanical Engineering, Université de Sherbrooke, 2500 Boulevard de l'Université, Sherbrooke, Québec J1K 2R1, Canada*

ABSTRACT:
This article proposes a hybrid numerical-analytical approach to effectively predict the sound absorption coefficient of complex periodic metamaterials with a reasonably low computation time. A variation of an existing metamaterial, consisting of a periodic succession of necks and cavities, is also proposed. The design variation was intended to decrease the frequencies of the absorption coefficient resonant peaks and consists in adding eccentricity in the neck position. The hybrid approach combines a thermoviscous-acoustic (TVA) approach with the transfer matrix (TM) method. The TVA approach estimates the thermoviscous losses of acoustic waves in a periodic unit cell (PUC) of the metamaterial. The TM method is used to simulate the acoustic behaviour of the complete metamaterial from the TM of the PUC calculated numerically. The approach is compared to impedance tube measurements on prototypes of the metamaterial. The comparison shows that the proposed approach is in good agreement with the measured sound absorption coefficient. In addition, numerical simulations and experiments demonstrate that the proposed variation of the existing metamaterial results in a shift of the absorption peaks down in frequency without deteriorating their sound absorption performance.
 https://doi.org/10.1121/10.0006441
(Received 21 January 2021; revised 18 August 2021; accepted 3 September 2021; published online 29 September 2021)
[Editor: David E. Scarborough] Pages: 2272–2281

I. INTRODUCTION

The attenuation of low frequency noise in small cavities is an important problem in certain industrial applications (muffler, gas turbine combustion chamber, aircraft engine, and aircraft panel). The long acoustic wavelengths associated with the low frequencies of interest determine the main design constraints for the problem under study. For this frequency range, conventional thin acoustic layers exhibit a low sound absorption. As a general rule, to improve the sound absorption using conventional materials, a large material thickness is required. Thus, for applications in which the volume available for sound absorbing materials is limited, new innovative designs of thin and light acoustic materials, which are effective at low frequencies and can withstand a harsh environment, are needed. One solution to this problem is the use of acoustic metamaterials. Acoustic metamaterials are structured arrangements of elementary, generally periodic, structures (e.g., arrays of acoustic or elastic resonators or phononic crystals) whose characteristic size is very small compared to the acoustic wavelength.[1] The metamaterial makes it possible to control or manipulate the propagation of the acoustic wave by a careful combination of these elementary structures in order to make its equivalent density and compressibility negative.[1–5]

Dengke *et al.*[2] used tubes of different depths in parallel to improve the low frequency sound absorption. Wang *et al.*[6,7] investigated the coupling effect of the parallel–arranged micro-perforated panels with different air cavities and concluded that multi-resonant systems have the potential to improve the bandwidth of the sound absorption. Aurégan *et al.*[8,9] presented a thin subwavelength metamaterial embedded in an airflow channel. The material used was made of a series of thin rectangular tubes mounted in parallel on the inner surface of the airflow channel. They showed that this optimized material gives a significant attenuation at low frequencies. This material has proven to be a possible solution for air flow channels when space constraints and low frequency noise render quarter wave resonators unusable. Based on the works of Bradley,[10] Leclaire *et al.*[11] studied a structured perforated material containing periodically spaced dead-end pores (such as quarter wavelength or Helmholtz resonators). In Ref. 11, it was proposed to model the resonant material with periodically spaced dead-end cavities by a transfer matrix method (TMM) with a low frequency asymptotic approach. It has been shown that the presence of the dead-end pore network at low frequencies

[a)]Electronic mail: TenonCharly.Kone@nrc-cnrc.gc.ca
[b)]ORCID: 0000-0002-6718-0339.
[c)]ORCID: 0000-0003-0058-6315.

https://doi.org/10.1121/10.0006441

results in an increased effective compressibility of the material without modifying its effective dynamic density. In turn, this induces a decrease in the effective sound speed in the material, which is responsible for the decrease in the acoustic resonance frequencies. Based on the work of Leclaire, Dupont *et al.*[12] proposed a new microstructure for the design of low frequency resonant acoustic absorbers. A perforated material was studied in which the main perforations were connected to a collection of periodically spaced very thin annular dead-end pores with respect to the lateral size. This solution consisted in connecting dead-end pores, i.e., thin cavity resonators, on a main tubular pore to create dead-end porosity materials. One of the advantages of this metamaterial design was to shift the absorption peaks toward the low frequencies. This can be explained by an increase in the effective compressibility of the material, thanks to both the effective compressibility and the volume of the area added in the cavities. These two parameters are responsible for reducing the effective speed and, therefore, the acoustic natural frequencies of the material.[12]

Although these studies have demonstrated the growing potential of metamaterials, most of them have used analytical methods, such as a lumped approach with the TMM, or the finite element method (FEM) to solve the acoustic Helmholtz equation in the fluid phase of the metamaterials. The equivalent fluid model, such as the Johnson-Champoux-Allard (JCA) model,[13] was used to account for thermoviscous losses in the metamaterials by calculating an effective dynamic density and bulk modulus (compressibility) for the air in the metamaterials. These methods have shown good agreement with experiments for simple geometries for which the analytical calculation of the effective properties is possible. However, even for materials with relatively simple geometries, such as perforated multipancake cavities, the approaches reached their limits beyond the first absorption peak.[12] For example, for the metamaterials presented by Dupont *et al.*,[12] the predictions using the JCA model are only precise for the first resonance peak (about 400 Hz for a cylinder 31 mm in length and 44.44 mm in diameter) but not entirely satisfactory at higher frequency resonance peaks (1100 Hz for the second peak) regardless of the methods used (analytical and numerical). In fact, the JCA model evaluates the effective properties of the air in the metamaterials with the geometric parameters of the cylindrical and/or slit pores. It does not make it possible to correctly evaluate the effective properties of the air in complex shaped metamaterials.[12–14] In addition, the absorption properties of these metamaterials are not yet satisfactory for aeronautical applications for which the available volume for the implementation of the acoustic absorber could be very small (e.g., gas turbine combustion chamber, aircraft engine, and aircraft panel).

This article (i) explores a more complex geometric variant of the metamaterial proposed by Dupont *et al.*[12] to reduce its resonant frequencies, (ii) proposes a hybrid numerical-analytical modeling method to consider more precisely the thermoviscous losses in metamaterials, and (iii) experimentally validates the variant of the metamaterial and modeling method on the prototypes. To accurately calculate the effective properties of the air in metamaterials, it is proposed to use the numerical thermoviscous-acoustic (TVA) simulations instead of the JCA analytical model as was performed in previous works. As such simulations take time, it is proposed to solve the TVA problem only on a periodic unit cell (PUC) of the metamaterial to deduce its transfer matrix (TM). Then, to construct the complete TM of the metamaterial, it is proposed to use the TM of the unit cell in the analytical TMM. We believe that such a hybrid approach is more suited to the study of a very large number of metamaterial configurations. This is because a PUC TM database can be developed using the TVA method, and then a large number of cell combinations can be quickly calculated by the TMM.

The article is structured as follows. Section II gives a description of the two metamaterials studied. Section III describes the equations of the TVA problem to be solved and presents the hybrid thermoviscous-acoustic and transfer matrix (TVA-TM) method to derive the TM of the metamaterials from the solution of the TVA problem on a PUC representation of the metamaterials. Section IV compares the sound absorption coefficients at normal incidence obtained by the hybrid TVA-TM method with measurements obtained with an impedance tube on prototypes of the metamaterials.

II. MATERIALS

One of the main objectives of this study is to develop metamaterials with complex geometries capable to effectively attenuate the acoustic waves at low frequencies within a limited available physical integration volume. Two metamaterial geometries are studied: centered neck metamaterial, also referred to as simple geometry, and off-centered neck metamaterial, also referred to as complex geometry. The computer-aided design (CAD) models of both the simple and complex geometries are shown in Fig. 1. Each metamaterial was studied in normal-incidence sound absorption with a rigid wall backing condition. The necks are all cylindrical and of the same diameter $d = 3.51$ mm and thickness $\ell = 3.59$ mm. The cavities are also all cylindrical and of the same diameter $D = 42.40$ mm and thickness $L = 3.83$ mm.

A. Centered neck metamaterial

The centered neck metamaterial is similar to the metamaterial proposed by Dupont *et al.*[12] and was simulated analytically, using the TMM and numerically, using the FEM. In their study, the thermoviscous losses were modeled using the equivalent fluid approach described by the JCA model. In the method proposed in this article, these losses are obtained directly by solving the Navier-Stokes equations of the TVA problem described in Sec. III. This metamaterial may best be described as a series network of Helmholtz resonators, i.e., concentric necks and cavities on the same axis

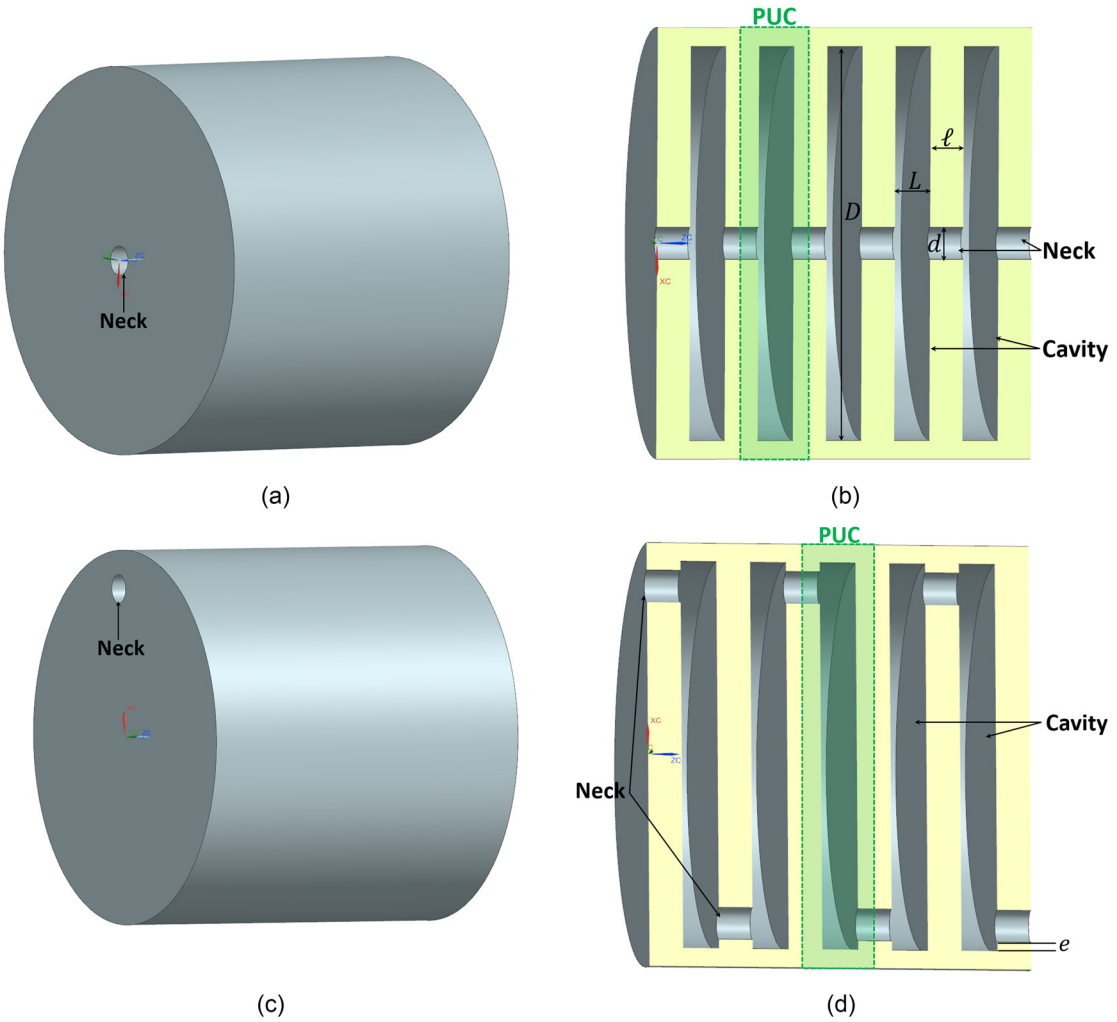

FIG. 1. (Color online) The CAD models of the centered neck (top) and off-centered neck (bottom) metamaterials. The full geometry view (left) and half geometry cut view (right) are shown.

of revolution [Figs. 1(a) and 1(b)]. The number of neck-cavity successions defines the metamaterial. The centered neck metamaterial geometry is axisymmetric and allows a two-dimensional (2D) axisymmetric numerical modeling with the FEMs.

B. Off-centered neck metamaterial

The off-centered neck metamaterial is similar to the first one, but the necks are off-centered and diametrically opposed [Figs. 1(c) and 1(d)]. Here, all of the cavities have the same axis of revolution. However, the axes of the necks are at a radial distance $(D-d)/2-e$ (with $e=1$ mm) from the axis of revolution of the cavities. This off-centered configuration makes it possible to increase the thermoviscous losses and length of the wave propagation path. It is, thus, hoped to reduce the resonance frequencies compared to the centered case. This geometry is not axisymmetric and, therefore, does not allow an axisymmetric 2D numerical modeling. However, it has a symmetry plan, which allows for the numerical modeling of only half of the three-dimensional (3D) geometry.

C. Prototype manufacturing

Figure 2 shows pictures of the manufactured metamaterial prototypes. The manufacturing was performed by computer numerical control (CNC) machining with a standard tolerance of ± 0.125 mm on all dimensions and a surface finish International Organization for Standardization (ISO) grade N8 (Ra $= 3.2\,\mu$m). The material used is aluminum 6061-T6. A preliminary numerical calculation on a plate (44.40-mm diameter and 3.59-mm thick), clamped on its circumference, showed that the first elastic resonance (18.9 kHz) of the prototypes is greater than the measured frequency range of interest in this investigation. Consequently, the elastic resonance of each prototype did not interfere with its meta-acoustical behaviour as was the case in the study by Dupont *et al.*.[12]

The prototype metamaterial consisted of one to six subassemblies. Each subset consisted of a single neck and a single cavity. The assembly ended with a rigid end plate containing a single neck. In addition, the outside diameter of the metamaterial is designed to fit into an impedance tube of diameter $D_T = 44.44$ mm. Finally, to facilitate the assembly (alignment and avoid leaks between parts), the design

https://doi.org/10.1121/10.0006441

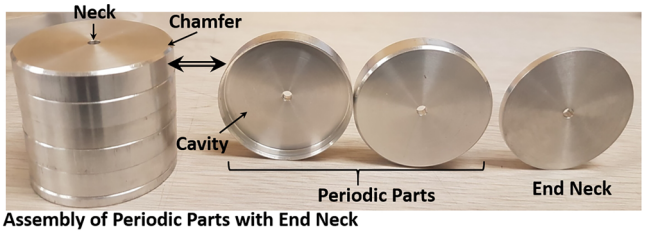

FIG. 2. (Color online) Photos of the manufactured parts and assemblies of the prototypes, showing the metamaterials with a centered neck (top) and off-centered neck (bottom).

includes a chamber (1 mm × 45 deg). Figure 2 shows assemblies for the centered and off-centered neck configurations in the case of 5 subassemblies terminated by a rigid end plate containing a single neck.

III. METHODS

The use of the equivalent fluid model (JCA) as implemented in the work by Dupont *et al.*[12] does not correctly predict the acoustic properties of the metamaterials with complex geometries. A new hybrid approach to calculate the acoustic absorption coefficient at normal incidence is proposed. This hybrid approach is based on the coupling of the solution of the Navier-Stokes equations (TVA) and TM method. Here, the approach proposed is referred to as the hybrid TVA-TM.

A. TVA approach

The TVA wave propagation is part of the problem of fluid dynamics. Under the continuum assumption, it can be modeled by the Navier-Stokes equations. The governing equations for TVA in the frequency domain (with time convention $e^{i\omega t}$) are comprised of the continuity equation, momentum equations, energy conservation equation, and linearized equation of state.[15] They are, respectively, given by

$$i\omega\rho + \nabla\cdot(\rho_0\mathbf{u}) = 0, \tag{1}$$

$$i\omega\rho_0\mathbf{u} = \nabla\cdot\left[-pI + \mu\left(\nabla\mathbf{u} + (\nabla\mathbf{u})^T\right) - \left(\frac{2}{3}\mu - \mu_B\right)(\nabla\cdot\mathbf{u})I\right], \tag{2}$$

$$i\omega(\rho_0 C_p T - T_0\alpha_0 p) = -\nabla\cdot(k\nabla T) + Q, \tag{3}$$

$$\rho = \rho_0(\beta_T p - \alpha_0 T), \tag{4}$$

where ω is the angular frequency of the harmonic excitation, ∇ and $\nabla\cdot$ are the gradient and divergent operators, respectively, and ρ, T, p, and $\mathbf{u}$ are the instantaneous density, temperature, pressure, and velocity field of the fluid, respectively. The properties of the quiescent fluid (also referred to as the background properties) at temperature T_0 and pressure p_0 are the density ρ_0, dynamic viscosity μ, bulk viscosity μ_B, heat capacity at constant pressure C_p, thermal conductivity k, coefficient of thermal expansion (isobaric) $\alpha_0 = -(1/\rho_0)[\partial\rho_0/\partial T_0]_{p_0}$, and the isothermal compressibility $\beta_T = (1/\rho_0)[\partial\rho_0/\partial p]_{T_0}$. Q is a possible heat source. No heat source is considered in this study.

Equations (1)–(4) were solved using the TVA module of COMSOL Multiphysics software. In Secs. III B–V, the TVA module implemented in COMSOL[15] is used to determine the TM of a PUC of the metamaterials. The approach brings together the TVA module and acoustic pressure (PA) module of COMSOL.[15] The PA module solves the classical Helmholtz equation for acoustic problems. For clarity, the different stages of the implemented approach methodology will be illustrated through an application.

B. Hybrid TVA-TM approach

The proposed hybrid approach (TVA-TM) couples the PA method (acoustic Helmholtz equation), TVA method, and TM method. The objective is to rapidly predict the normal-incidence sound absorption coefficient of a complex metamaterial. Because the necks and cavities are small compared to the thermal and viscous skin depths and their geometry and the fluid path geometry may be complex, the analytical calculation of the effective properties of the fluid in the metamaterial may not be sufficiently accurate. For the centered neck metamaterial, Dupont *et al.*[12] showed that it is possible for this simple geometry to correctly calculate the effective properties using the JCA model. However, for arbitrary geometries, notably the off-centered neck metamaterial, it may be complicated or impossible. Consequently, the TVA method was used to account for thermoviscous losses on the wave propagation in complex metamaterials.

Because numerical TVA requires fine meshing to converge, notably in the vicinity of the walls, the computation time may rapidly become important as the metamaterial becomes more complex. In our study, to limit the computation time, the numerical calculations were performed only for a single PUC. The PUCs for centered and off-centered metamaterials are shown in the sectional views of the CAD model in Figs. 1(b) and 1(d) and detailed in Fig. 3. For the centered geometry, a 2D axisymmetrical model of the PUC is used. For the off-centered geometry, a 3D half-symmetrical model of the PUC is used.

The objective of the numerical calculations is to calculate the TM $\mathbf{T}$ of the PUC, then to raise it to the power of N (subassembly number) to obtain the TM $\mathbf{T}_G$ of the metamaterial, and finally deduce the sound absorption coefficient of the metamaterial. To retrieve the TM of the PUC, the TVA

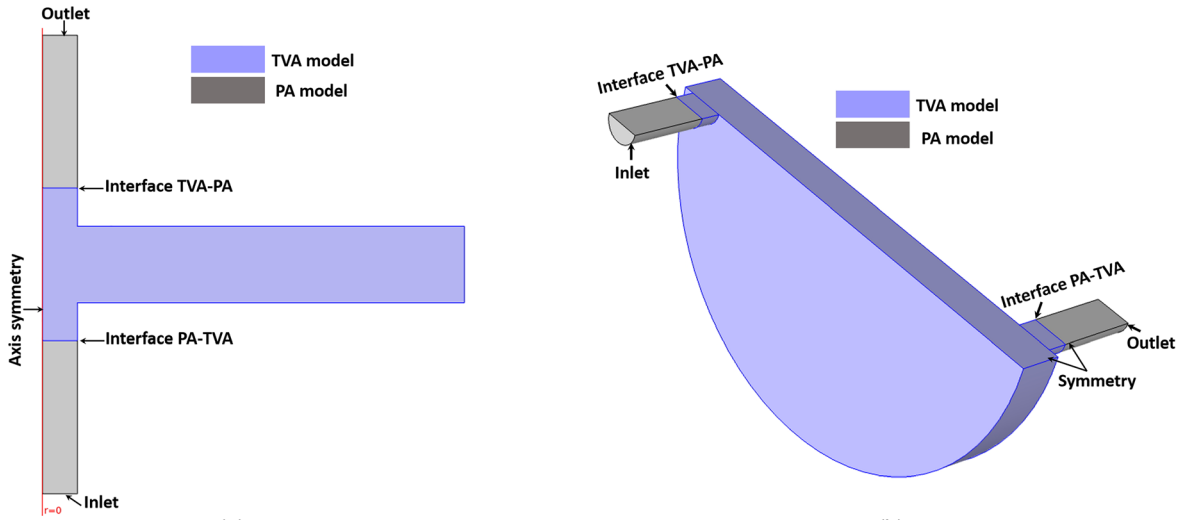

FIG. 3. (Color online) The PUCs of the metamaterials studied, showing the (a) 2D axisymmetrical PUC model for the centered neck metamaterial and (b) 3D half-symmetrical PUC model for the off-centered neck metamaterial.

problem is coupled to the PA problem as shown in Fig. 3. The PUC is modeled with the TVA (blue zone), and it is sandwiched between the acoustic inlet and outlet regions. Because these regions are not subject to thermoviscous losses of the metamaterial, they are modeled with PA (gray zones), having properties of quiescent air. These regions, where only the Helmholtz equation is solved, are necessary to ensure the reconstruction of plane waves far from the TVA–PA interfaces to be compatible with the underlying hypothesis of the TMM. This hypothesis is verified when the length of these regions is at least twice the diameter of the neck.[14]

To obtain the TM of the PUC of the metamaterial in the TVA region (cavity and the two half-length adjacent neck segments), the calculation is made in two steps using two different inlet and outlet boundary conditions. In a first step, the inlet pressure and outlet axial acoustic velocity were specified, whereas in the second step, the inlet axial velocity and outlet pressure were specified. For each step, the thermoviscous-acoustic–acoustic pressure (TVA-PA) problem was solved to obtain the averages of the acoustic pressures and axial velocities at the PA–TVA and TVA–PA interfaces shown in Fig. 3. These averaged inlet $(\bar{p}_i, \bar{u}_i)$ and outlet $(\bar{p}_o, \bar{u}_o)$ acoustic fields are linked by the TM of the PUC by

$$\begin{pmatrix} \bar{p}_i \\ \bar{u}_i \end{pmatrix} = \mathbf{T} \begin{pmatrix} \bar{p}_o \\ \bar{u}_o \end{pmatrix}, \tag{5}$$

where $\mathbf{T} = [T_{11}, T_{12}; T_{21}, T_{22}]$. This TM is a 2×2 matrix with four coefficients. With the two-step calculations and eight averaged pressures and velocities, Eq. (5) yields four equations to determine the four matrix coefficients as follows:

$$T_{11} = \frac{\bar{p}_{i_{\text{step1}}} \bar{u}_{o_{\text{step2}}} - \bar{p}_{i_{\text{step2}}} \bar{u}_{o_{\text{step1}}}}{\bar{p}_{o_{\text{step1}}} \bar{u}_{o_{\text{step2}}} - \bar{p}_{o_{\text{step2}}} \bar{u}_{o_{\text{step1}}}}, \tag{6a}$$

$$T_{12} = \frac{\bar{p}_{i_{\text{step2}}} \bar{p}_{o_{\text{step1}}} - \bar{p}_{i_{\text{step1}}} \bar{p}_{o_{\text{step2}}}}{\bar{p}_{o_{\text{step1}}} \bar{u}_{o_{\text{step2}}} - \bar{p}_{o_{\text{step2}}} \bar{u}_{o_{\text{step1}}}}, \tag{6b}$$

$$T_{21} = \frac{\bar{u}_{i_{\text{step1}}} \bar{u}_{o_{\text{step2}}} - \bar{u}_{i_{\text{step2}}} \bar{u}_{o_{\text{step1}}}}{\bar{p}_{o_{\text{step1}}} \bar{u}_{o_{\text{step2}}} - \bar{p}_{o_{\text{step2}}} \bar{u}_{o_{\text{step1}}}}, \tag{6c}$$

$$T_{22} = \frac{\bar{p}_{o_{\text{step1}}} \bar{u}_{i_{\text{step2}}} - \bar{p}_{o_{\text{step2}}} \bar{u}_{i_{\text{step1}}}}{\bar{p}_{o_{\text{step1}}} \bar{u}_{o_{\text{step2}}} - \bar{p}_{o_{\text{step2}}} \bar{u}_{o_{\text{step1}}}}. \tag{6d}$$

Now, knowing the TM of the PUC, the global TM of the metamaterial constituted of N cells, stacked in series, is deduced from the classical TMM[14] given by

$$\mathbf{T}_G = \mathbf{T}^N. \tag{7}$$

To consider a total length at the inlet and outlet of the assembled metamaterial, it is necessary to pre-multiply and post-multiply the TM T_G by the TM of a half neck T_C. Here, this matrix T_C is computed analytically according to the equivalent fluid approach with

$$\mathbf{T}_C = \begin{pmatrix} \cos(k_e \ell/2) & jZ_e \sin(k_e \ell/2) \\ \frac{j}{Z_e} \sin(k_e \ell/2) & \cos(k_e \ell/2) \end{pmatrix}, \tag{8}$$

where k_e and Z_e are the effective complex wave number and characteristic impedance of the fluid in the half neck. They are calculed with the JCA model[13] and corresponding neck parameters given in Table I. Thus, the global TM T_G of the metamaterial becomes

$$\mathbf{T}_G = T_C \mathbf{T}^N T_C. \tag{9}$$

To take into account the change of the cross section between the upstream medium (for example, impedance tube) and the first neck of the metamaterial, and eventually between a downstream medium (for example, transmission

https://doi.org/10.1121/10.0006441

TABLE I. The JCA parameters of the half neck with η as the dynamic viscosity of air.

Viscous characteristic length Λ (mm)	Thermal characteristic length Λ'(mm)	Tortuosity α_∞	Static airflow resistivity σ (P_a s/m^2)	Open porosity Φ (%)
$d/2$	$d/2$	1	$32\eta/d^2\Phi$	100

tube) and the end neck of the metamaterial, the global matrix is modified as

$$\mathbf{T}_G = \mathbf{T}_o T_C \mathbf{T}^N T_C \mathbf{T}_o^{-1}, \tag{10}$$

where $\mathbf{T}_o = [1, 0; 0, r]$, and r is the surface ratio between the neck and the surrounding medium. Here, it is assumed that the upstream and downstream media have similar surface areas. For instance, if the metamaterial is tested in a circular impedance tube of diameter D_T, then $r = (d/D_T)^2$.

For the rigidly backed sample configuration (sound absorption configuration), the main pore is open at one side and closed at the other side. At the closed end termination of main pore, r tends to infinity and then the global matrix for this configuration is given by

$$\mathbf{T}_G = \mathbf{T}_o T_C \mathbf{T}^N T_C \mathbf{T}_1, \tag{11}$$

where $\mathbf{T}_1 = [1, 0; 0, 0]$, indicating the transmission matrix for the closed boundary.

Finally, by defining the global matrix as $\mathbf{T}_G = [T_{G_{11}}, T_{G_{12}}; T_{G_{21}}, T_{G_{22}}]$, the normal-incidence sound absorption coefficient is given by

$$\alpha = 1 - \left| \frac{T_{G_{11}} - T_{G_{21}} Z_o}{T_{G_{11}} + T_{G_{21}} Z_o} \right|^2, \tag{12}$$

where Z_o is the acoustic impedance of the quiescent fluid (here, it is air).

IV. RESULTS

A. Model setup

The PUC models described in Sec. III were used in the numerical simulations. For the centered metamaterial, an axisymmetrical boundary condition was used on the revolution axis of its 2D PUC model shown in Fig. 3(a). For the off-centered metamaterial, a symmetry condition was used on the symmetry plan of its 3D PUC model shown in Fig. 3(b). Excluding the inlet and outlet faces, the no-slip and isothermal boundary conditions were used on all of the other faces. The arbitrary values of the imposed acoustic pressures and axial velocities at the inlet and outlet for the two-step calculation are presented in Table II. Finally, parabolic triangular elements were used to mesh the acoustic domain. The mesh includes boundary layer meshes in the metamaterial PUC zone. The convergence of the numerical simulation results was verified in the frequency range of interest by the mesh refinements. At most, 16 h of computation were necessary to deduce the TM of a PUC cell by the TVA approach instead of $N \times 16$ h for a metamaterial of N cells. Here, the TM was calculated at frequencies ranging from 10 to 2000 Hz.

B. Experimental setup

To validate the numerical simulation results, the measurements were conducted with a Mecanum's impedance tube. The diameter of the impedance tube is 44.44 mm. The two-microphone method[16] was used. The valid frequency range for the setup was between 115 and 4300 Hz (upstream microphone spacing is 30 mm). The sound pressure excitation was a random noise with a global sound pressure level of 90 dB at the microphones. The manufactured parts shown in Fig. 2 were assembled in the tube to form the metamaterial. The metamaterial was backed by the rigid end of the tube. Each metamaterial was tested three times following a disassembly and reassembly procedure of the different parts. This made it possible to obtain a measurement dispersion envelope that is defined by the minimum and maximum values at each frequency. Four centered neck and one off-centered neck metamaterial configurations were tested. Each tested configuration consisted in a serial assembly of identical periodic cells, where the number N of cells varied ($N = 3$, 4, 5, and 6).

C. Results

The measured and numerically simulated predictions of the normal-incidence sound absorption coefficient [Eq. (12)] for each metamaterial are presented in Fig. 4, for centered neck metamaterials and in Fig. 5 for the off-centered neck metamaterials. In Figs. 4 and 5, the gray envelopes correspond to the impedance tube measurements, whereas the red solid lines correspond to the hybrid TVA-TM method proposed in Sec. III. In addition, a third comparison was considered, represented by the dashed blue lines and corresponding to a finite element calculation on the whole geometry (not only on a PUC as for the TVA-TM method), where only the Helmholtz PA equation is solved. In this case, the fluids in the necks and cavities are described by equivalent fluids to account for the thermoviscous losses. Here, the JCA equivalent fluid model is used. It results in equivalent fluid properties for circular pores in the necks

TABLE II. The values of acoustic fields imposed at the inlet and outlet for the two-step calculation.

Step	1		2	
Boundary	Inlet	Outlet	Inlet	Outlet
Pressure (Pa)	1			0
Axial velocity (m/s)	—	0	1	—

and parallel slits in the cavities. This pressure acoustic–Johnson-Champoux-Allard (PA-JCA) FEM approach is described in Sec. 4.1.2 of Ref. 12. It is presented here to show the limitation of such an approach to account for thermoviscous losses when the geometry is more complex.

V. DISCUSSION

In Figs. 4 and 5, one can note that for all of the cases above 1650 Hz, the normal-incidence sound absorption coefficient drops to zero. This is related to the start of the so-called first stop band, which is related to the first quarter wavelength resonance of the annular cavities of the metamaterial.[12,17] For the design under study, this resonant frequency is 2694 Hz, and the start of the stop band appears just after the Nth resonance of the metamaterials.

In addition, it has been shown in Refs. 11 and 12 that this metamaterial can be modeled as a homogeneous equivalent fluid characterized by equivalent properties (such as speed of sound, density, compressibility, and wave number). This equivalent modeling is valid until the start of the stop band. Thus, just as for an equivalent fluid (or a typical porous material), absorption peaks appear at odd multiples n of the quarter wave resonance[4,11,12,18] given by

$$f_{\text{peak},n} = n\frac{\text{Re}(c_{\text{eq},n})}{4L_t}, \tag{13}$$

where $n = (1, 3, 5, \ldots)$, L_t is the total thickness of the metamaterial, and $c_{\text{eq},n}$ is the equivalent sound speed. It can be noted that $c_{\text{eq},n}$ depends on n (this means that it depends on the frequency). As an indication, the surface distributions of the acoustic pressure for the first four quarter wave resonances are illustrated in Fig. 6 for the case of the metamaterial with $N = 6$ PUCs. On the right in Fig. 6, the distribution of the pressure along the axisymmetric axis is shown. Note that the pressure on the incident side (bottom) is close to 0 Pa while the pressure derivative with respect to the axis is zero at the closed end. These pressure distributions were obtained with the PA-JCA FEM approach that was discussed earlier.

A. Centered neck metamaterial

Regardless of the number N of cells of the metamaterial, the agreement between the hybrid TVA-TM approach and the experimental results are good, mainly for the first absorption peaks. For the last absorption peaks, the peaks predicted by the model are slightly shifted upward in the frequency, and their amplitudes are slightly underestimated. The results clearly show the effects of the number of periodic cells. By increasing the number of cells, the ith peak move toward low frequencies. This is due to the increase in the total volume of the metamaterial and, in particular, the volume of the cavities. Also, it is worth mentioning that the number of peaks up to the stop band is given by the number N of cells. In addition, the central frequency at which the stop band arises is not related to the number of cells nor to the total thickness of the metamaterial. Indeed, the stop band depends on the cavity resonance frequency (here, close to 2694 Hz) and periodic spacing between cavities.[17] For each tested sample, the geometries of the cavities and spacing between the cavities remain the same. Consequently, the same stop band is observed for all of the samples.

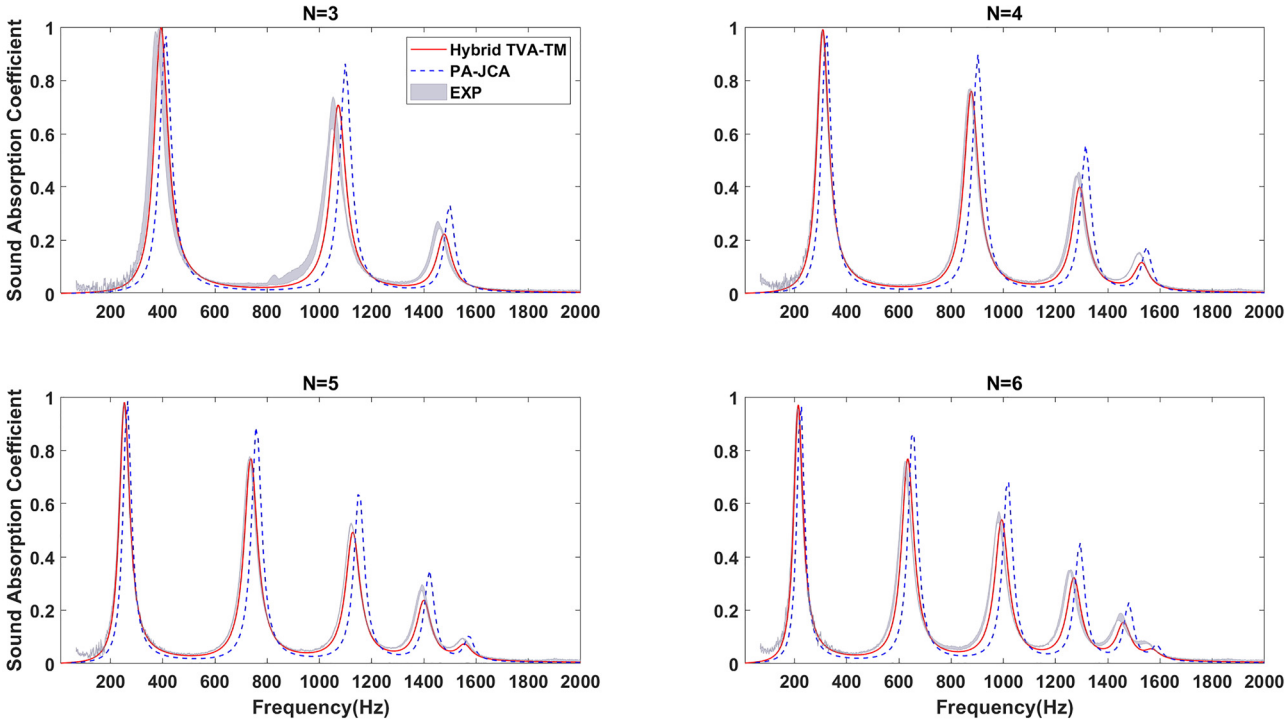

FIG. 4. (Color online) The normal-incidence sound absorption coefficient of the centered neck metamaterial, as well as the comparisons between the measurements and predictions for different numbers N of cells are shown.

https://doi.org/10.1121/10.0006441

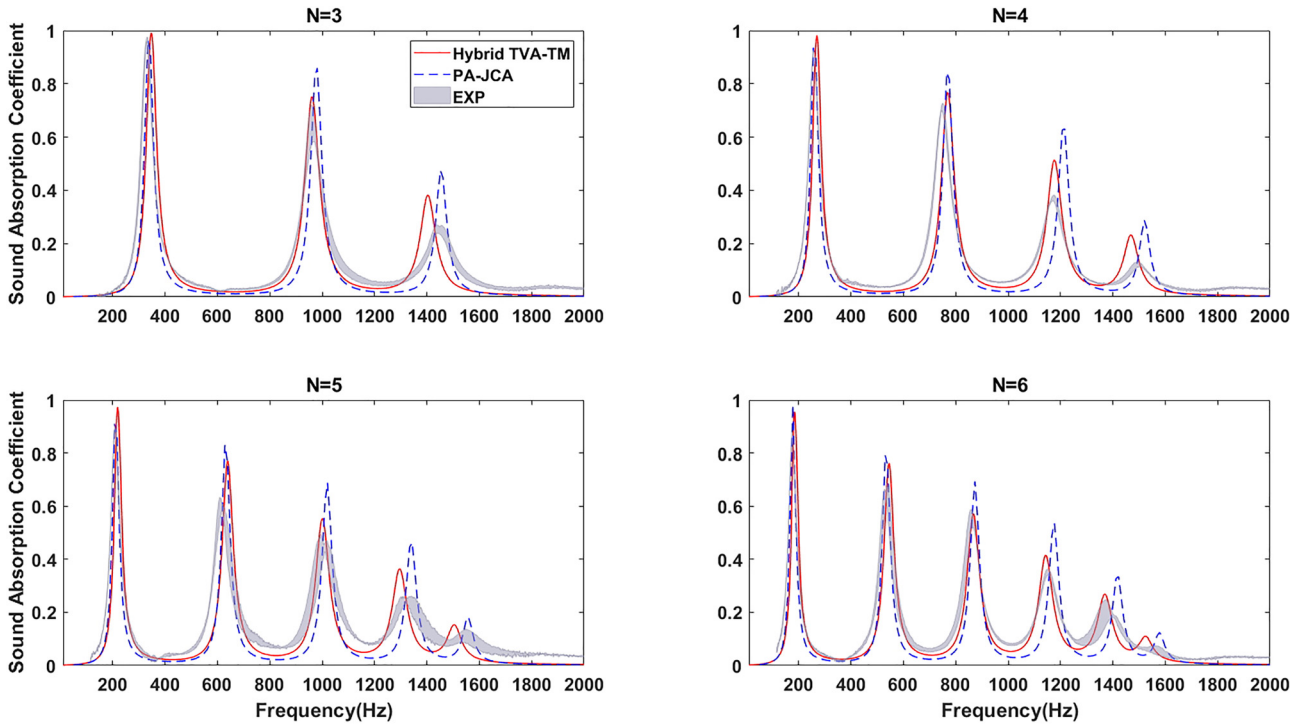

FIG. 5. (Color online) The normal-incidence sound absorption coefficient of the off-centered neck metamaterials, as well as the comparisons between the testing and numerical prediction results for different numbers N of cells are shown.

In the dips of the curves, mainly at higher frequencies, the hybrid model slightly underestimates the sound absorption coefficient compared to the measurements. The authors believe that this may be caused by the roughness of the surface sample and Knudsen scattering.

In general, the proposed hybrid approach gives better results than the PA-JCA approach regardless of the metamaterial. This is due to the fact that thermoviscous losses are explicitly calculated with the TVA for the real geometry and not approximated by circular and slit pore geometries as in the JCA equivalent fluid approach. Therefore, even for this relatively simple geometry, the TVA-TM approach is preferable to the PA-JCA approach.

B. Off-centered neck metamaterial

Like the centered neck metamaterial, the off-centered neck metamaterial is tested with cells $N = 3$, 4, 5, and 6 as shown in Fig. 5. Again, the TVA-TM hybrid approach compares well to the impedance tube measurements.

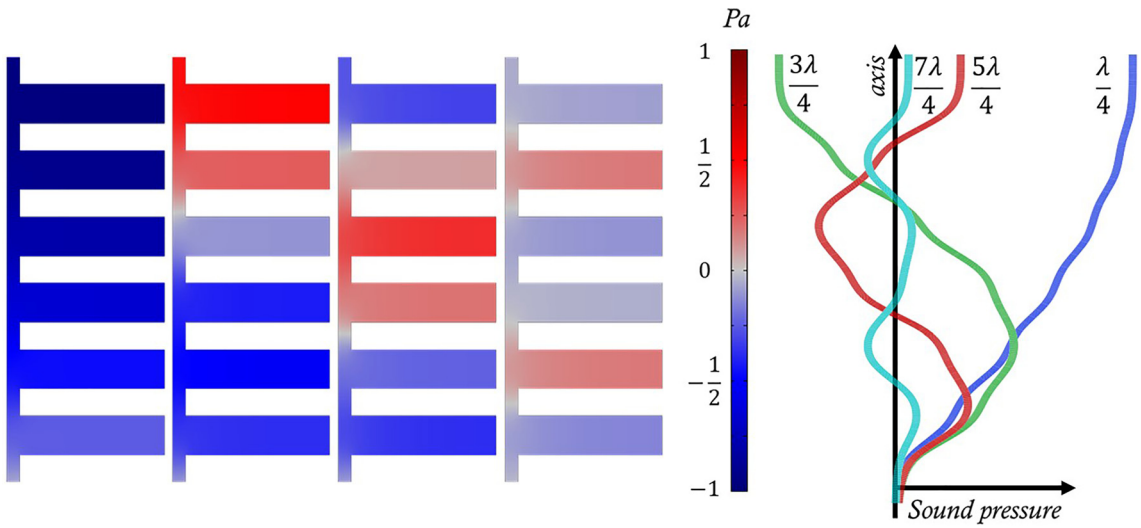

FIG. 6. (Color online) The sound pressure distribution of the axisymmetrical metamaterial with six PUCs for the first four resonant frequencies. From left to right, the first resonance at $\lambda/4$, second resonance at $3\lambda/4$, third resonance at $5\lambda/4$, and fourth resonance at $7\lambda/4$, and on the right, the distribution of the sound pressure along the axis of the metamaterial at the corresponding resonances are shown.

The comparison is better for the first peaks than for the last peaks. In the measurements, we observe more dispersion between different measurements of the same sample in the last peaks at higher frequencies. This dispersion comes from unmounting and mounting the samples between the tests. Unlike the centered neck case, the eccentric neck case adds additional complexity when assembling the parts to ensure that two successive necks are diametrically opposed. Again, at higher frequencies, the absorption coefficients predicted at the troughs are underestimated. For the same reason given above, we think this is due to the Knudsen diffusion occurring experimentally on the surfaces of the samples. This time, this diffusion is more important than in the case of the centered neck because the actual length of the acoustic path is greater due to the eccentricity of the necks.

Similar to the centered neck case, the same conclusions apply for the off-centered case: (1) the number of periodic cells defines the number of absorption peaks, and (2) the dimensions of the periodic cell (not its number) defines the beginning of the stop band. Because the dimensions of the necks and cavities are the same between the centered and off-centered cases, the same stop band is observed. It seems that the eccentricity of the necks, increasing the equivalent tortuosity of the medium, does not affect the stop band. This eccentricity mainly affects the position of the sound absorption coefficient peaks.

Finally, even if the PA-JCA approach gives relatively good predictions, it diverges more when compared to the measurements than in the hybrid TVA-TM approach. Surprisingly, it seems that even with the eccentricity of the necks, the effective JCA properties of the air in the necks and cavities are relatively well reproduced with the pore and slit models as proposed by Dupont *et al.*[12] for the centered neck case. This leads to almost the same accuracy of the PA-JCA predictions for centered and off-centered neck metamaterials. Even with an eccentricity, the configuration of the metamaterials is relatively simple and the PA-JCA gives acceptable predictions. However, the TVA-TM approach is more precise for finely capturing the thermoviscous losses. It can be expected that with a more complex geometry, the PA-JCA predictions will start to diverge more as compared to the measurements, whereas the accuracy of the TVA-TM predictions will not be affected.

C. Comparison between centered and off-centered neck metamaterials

Figure 7 compares the calculated normal-incidence sound absorption coefficients of the centered neck metamaterial with the off-centered neck metamaterial for $N = 3$, 4, 5, and 6. For a given number of cells N, both of the metamaterials have the same volume of air and the same total sample thickness. It can be observed that the eccentricity of the necks causes a displacement of the absorption peaks toward the low frequencies. This can be viewed as an increase in the acoustic path in the medium and, hence, by an increase in its equivalent tortuosity. The displacement toward the low frequencies is more important for the intermediary peaks. Typically, the reduction in frequency at the second peak is about 50% greater than the reduction in frequency at the first peak. Although the eccentricity moves the absorption peaks down in frequency, it only slightly affects the peak amplitudes of the sound absorption coefficient. Indeed, the amplitudes of the first peaks remain almost unchanged,

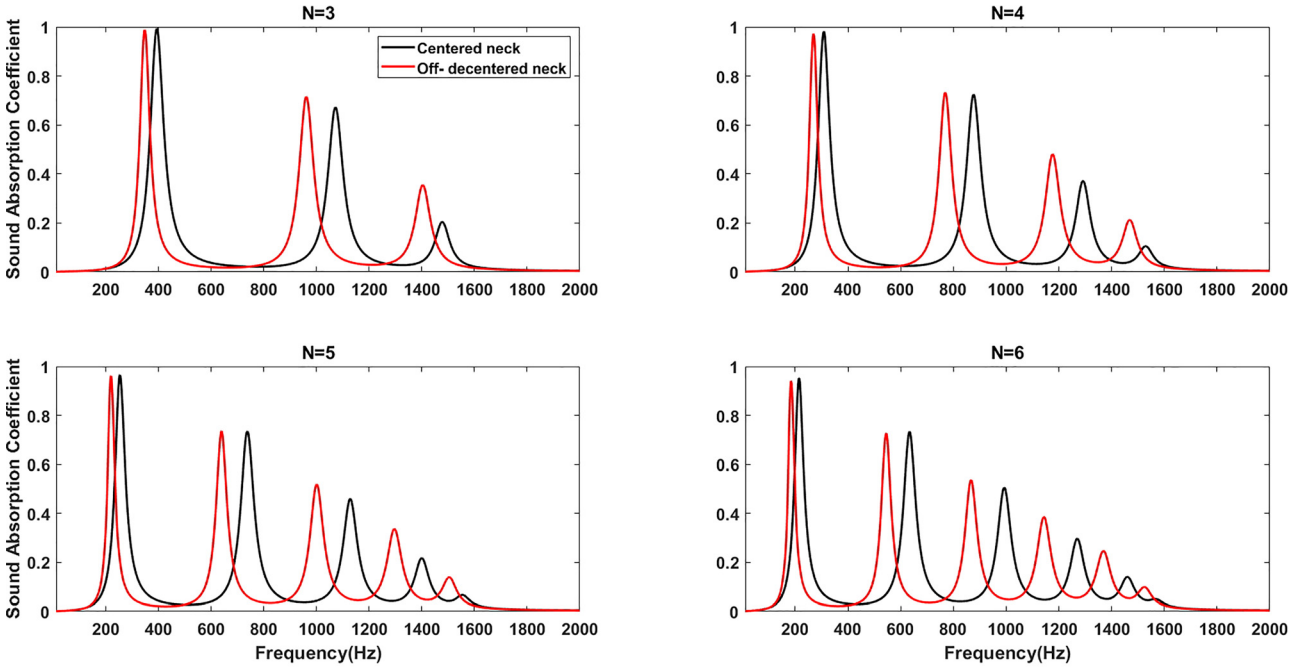

FIG. 7. (Color online) The normal-incidence sound absorption coefficient and the comparisons between the centered neck and off-centered neck metamaterials for different numbers N of periodic cells are shown. The results are obtained with the proposed hybrid TVA-TM approach.

and they are improved at the last peaks by the eccentricity. In addition, for the two metamaterials, it seems that the amplitude of the absorption coefficient at the peaks decreases, almost linearly, with the frequency.

VI. CONCLUSION

This article has proposed a hybrid approach to predict the sound absorption coefficient of a metamaterial made of a periodic succession of necks and cavities. The hybrid approach combines a numerical TVA problem applied to a PUC of a periodic metamaterial with the TM method. The metamaterial is a variation of the periodic centered neck-cavity metamaterial proposed by Dupont *et al.*,[12] consisting of adding eccentricity in the position of the necks. Whereas the TVA is solved to accurately take into account thermoviscous losses of the acoustic waves in the metamaterial and deduce the TM of the PUC, the TM method is used to build the full metamaterial with at most six periodic cells. The predictions obtained by the proposed method have been compared to the impedance tube measurements on prototypes of the metamaterial and a numerical simulation based on the equivalent fluid approach.

Compared to the equivalent fluid approach, the results have shown that the proposed hybrid TVA-TM approach better predicts the complex thermoviscous losses in the metamaterial. Its predictions are in very good agreement with the sound absorption coefficients measured using an impedance tube method. Moreover, the results have shown that the eccentricity added to the neck position allows for reducing the frequencies of all of the absorption peaks compared with the case without eccentricity and does not reduce the amplitude of the absorption peaks. In addition, the eccentricity of the neck position does not affect the beginning of the stop band effect on the absorption coefficient.

Compared to other numerical methods, the proposed approach optimally applies to the periodic metamaterial of a complex shape without making strong approximations on the thermoviscous losses. The fact that only the PUC is modeled allows the assembly of multiple PUC transfer matrices with a reduced computation time and rapidly creates metamaterials of different kinds and simulates their sound absorption performance using the TMM. The reduction in the computation time, compared to a full numerical analysis, makes the proposed hybrid method well suited for implementation in an optimisation procedure.

Finally, it should be mentioned that the authors believe that the additional absorption observed experimentally, compared to the predictions, can occur due to the roughness of the surface by the Knudsen diffusion. In addition, a certain dispersion was observed between successive measurements of the impedance tubes after the dismantling and reassembling of the samples, mainly at higher frequencies. This dispersion would be linked to the manufacturing and assembly tolerance of the metamaterial. Additional research on surface roughness and fabrication tolerance is needed to better understand this type of metamaterial.

ACKNOWLEDGMENTS

This research was partly supported by the Natural Sciences and Engineering Research Council of Canada (NSERC) and Siemens Canada Limited. Also, the authors wish to thank the "Ministère de l'économie et de l'innovation – Québec" (MEI), the Consortium for Research and Innovation in Aerospace in Québec (CRIAQ), and the Consortium for aerospace research and innovation in Canada (CARIC) for their financial support.

[1]Z. Liu, X. Zhang, Y. Mao, Y. Y. Zhu, Z. Yang, C. T. Chan, and P. Sheng, "Locally resonant sonic materials," Science **289**(5485), 1734–1736 (2000).
[2]L. Dengke, C. Doqing, and L. Bilong, "Enhancing the low frequency sound absorption of a perforated panel by parallel-arranged extended tubes," Appl. Acoust. **102**, 126–132 (2016).
[3]M. Yang, S. Chen, C. Fu, and P. Sheng, "Optimal sound-absorbing structures," Mater. Horiz. **4**, 673–680 (2017).
[4]L. Quan, Z. Xu, X. Liu, X. Gong, and P. A. Johnson, "Effective impedance boundary optimization and its contribution to dipole radiation and radiation pattern control," Nat. Commun. **5**(3188), 3188 (2014).
[5]L. Quan, X. Liu, and X. Gong, "Optimal sound-absorbing structures," J. Acoust. Soc. Am. **139**, 3373–3385 (2016).
[6]C. Q. Wang and L. X. Huang, "On the acoustic properties of parallel arrangement of multiple micro-perforated panels with different cavity depths," J. Acoust. Soc. Am. **130**, 208–216 (2011).
[7]C. Q. Wang, L. X. Huang, and Y. M. Zhang, "Oblique incidence sound absorption of parallel arrangement of multiple micro-perforated panels in a periodic pattern," Int. J. Acoust. Vib. **333**, 6828–6842 (2014).
[8]Y. Aurégan and M. Leroux, "Experimental evidence of an instability over an impedance wall in a duct with flow," Int. J. Acoust. Vib. **317**(3), 432–439 (2008).
[9]Y. Aurégan, M. Farooqui, and J.-P. Groby, "Low frequency sound attenuation in a flow duct using a thin slow sound material," J. Acoust. Soc. Am. **139**, EL149–EL153 (2016).
[10]C.-E. Bradley, "Time harmonic bloch wave propagation in periodic waveguides. Part I. Theory," Int. J. Acoust. Vib. **96**, 1844–1885 (1994).
[11]P. Leclaire, O. Umnova, T. Dupont, and R. Panneton, "Acoustical properties of air-saturated porous material with periodically distributed dead-end pores," J. Acoust. Soc. Am. **137**(4), 1772–1782 (2015).
[12]T. Dupont, P. Leclaire, R. Panneton, and O. Umnova, "A microstructure material design for low frequency sound absorption," Appl. Acoust. **136**(4), 86–93 (2018).
[13]Y. Champoux and J.-F. Allard, "Dynamic tortuosity and bulk modulus in air-saturated porous media," J. Appl. Phys. **70**(4), 1975–1979 (1991).
[14]J.-F. Allard and N. Atalla, *Propagation of Sound in Porous Media: Modeling Sound Absorbing Materials*, 2nd ed. (Elsevier Applied Science, New York, 2009).
[15]COMSOL, "Comsol: Acoustic module user's guide," available at https://doc.comsol.com/5.4/doc/com.comsol.help.aco/AcousticsModuleUsersGuide.pdf (Last viewed 9/22/2021).
[16]ASTME1050-12, "Standard test method for impedance and absorption of acoustical materials using a tube," in *Two Microphones and a Digital Frequency Analysis System*. (American Society for Testing and Materials, New York, 2012).
[17]X. Wang and C. M. Mak, "Acoustic performance of a duct loaded with identical resonators," J. Acoust. Soc. Am. **131**, EL316–EL322 (2012).
[18]R. Al Jahdali and Y. Wu, "Coupled resonators for sound trapping and absorption," Sci. Rep. **8**, 13855 (2018).